



# HHS Public Access

Author manuscript

*Proteomics*. Author manuscript; available in PMC 2021 March 01.

Published in final edited form as:

*Proteomics*. 2020 March ; 20(5-6): e1800406. doi:10.1002/pmic.201800406.

## Calcitriol prevents RAD51 loss and cGAS-STING-IFN response triggered by progerin

Nuria Coll-Bonfill<sup>1</sup>, Rafael Cancado de Faria<sup>1</sup>, Sweta Bhoopatiraju<sup>1</sup>, Susana Gonzalo<sup>1,\*</sup>

<sup>1</sup>Edward A. Doisy Department of Biochemistry and Molecular Biology, Saint Louis University School of Medicine, 1100 S Grand Blvd, St. Louis, MO 63104, USA

### Abstract

Hutchinson Gilford Progeria Syndrome (HGPS) is a devastating accelerated aging disease caused by *LMNA* gene mutation. The truncated lamin A protein produced “progerin” has a dominant toxic effect in cells, causing disruption of nuclear architecture and chromatin structure, genomic instability, gene expression changes, oxidative stress, and premature senescence. We previously showed that progerin-induced genomic instability involves replication stress (RS), characterized by replication fork (RF) stalling and nuclease-mediated degradation of stalled forks. RS is accompanied by activation of cGAS/STING cytosolic DNA sensing pathway and STAT1-regulated interferon (IFN)-like response. We also found that calcitriol, the active hormonal form of vitamin D, rescues RS and represses the cGAS/STING/IFN cascade. Here, we delve into mechanisms underlying RS in progerin-expressing cells and the rescue by calcitriol. We find that progerin elicits a marked downregulation of RAD51, concomitant with increased levels of phosphorylated-RPA (P-RPA), a marker of RS. Interestingly, calcitriol prevents RS and activation of the cGAS/STING/IFN response in part through maintenance of RAD51 levels in progerin-expressing cells. Thus, loss of RAD51 is one of the consequences of progerin expression that could contribute to replication stress and activation of the IFN response. Stabilization of RAD51 helps explain the beneficial effects of calcitriol in these processes.

### Introduction

To date, more than 450 mutations in the *LMNA* gene have been associated with degenerative disorders, broadly termed laminopathies, which include muscular dystrophies, neuropathies, lipodystrophies, and progeroid or premature aging diseases such as Hutchinson Gilford Progeria Syndrome (HGPS) [1, 2]. In addition, changes in the expression of lamins, especially downregulation, have been associated with poor prognosis in many cancers [3]. These data and the role of lamins in the maintenance of genome stability and function provide evidence for lamins functioning as “genome caretakers”. Although many studies

\*Corresponding author: Susana Gonzalo, Department of Biochemistry and Molecular Biology, St Louis University School of Medicine, 1100 S Grand Ave, St. Louis, MO 63104, USA, Phone: 314-9779244, sgonzalo@slu.edu.

Author contributions

N.C.B. and R.C.F. generated most of the data. S.B. performed some qRT-PCR experiments. S.G. supervised the research and prepared the manuscript. All authors read the manuscript and agreed to submit.

Declaration of interests

Authors declare no conflict of interest.

support that lamins are important for DNA repair, DNA replication, and telomere biology, the underlying mechanisms remain poorly understood [4, 5].

Our previous studies in progerin-expressing cells revealed accumulation of DNA damage and replication stress (RS) [6, 7]. In fact, the replication defects in progerin-expressing cells are more robust than in lamins-depleted cells, causing replication fork (RF) stalling in addition to fork degradation by nucleases [7]. Although the mechanisms underlying the detrimental effects of progerin in DNA replication are not fully understood, some studies have shown that progerin sequesters PCNA (Proliferating Cell Nuclear Antigen), a key factor in replication, away from the RF [8]. In addition, aberrant degradation of RFC1 (Replication Factor Complex 1) by serine proteases in progerin-expressing HGPS fibroblasts has been associated with defective loading of PCNA and Pol  $\delta$  onto DNA for replication [9]. RFC1 degradation and PCNA sequestration could explain the increase in RF stalling by progerin. In addition, we found that forks are susceptible to Mre11 nuclease-mediated degradation in progerin-expressing cells. As such, inhibition of Mre11 nuclease activity by Mirin rescues RF instability (RFI) [7]. This suggests that progerin might hinder not only replication fork progression by eliciting the mis-localization of replisome factors such as PCNA and RFC, but also the proper recruitment of RF protective factors during instances of RS.

Interestingly, our studies provided a link between RFI and activation of a cell-intrinsic innate immune response. We found that RS in progerin-expressing cells is accompanied by upregulation of the cGAS (cyclic-GMP-AMP synthase)-STING (stimulator of interferon genes) pathway of cytosolic DNA sensors and a STAT1-mediated interferon (IFN)-like response. Recently, cGAS, STING, and the downstream IFN response have been in the spotlight for their role in senescence/aging, cancer, and response to cancer immunotherapy [10, 11]. The view is that genomic instability due to DNA repair deficiencies, replication stress (RS), or exposure to genotoxic agents causes aberrant accumulation of self-DNA in the cytoplasm [11, 12, 13]. This is sensed by cGAS, which catalyzes the production of cGAMP. As a second messenger, cGAMP binds to STING, which undergoes a conformational change that activates TBK1 and IRF3 proteins, triggering the IFN response [14]. This cascade concludes with activation of pro-inflammatory programs such as the senescence-associated secretory pathway (SASP) that has dichotomous roles in aging and aging-related diseases such as cancer and cardiovascular disease [11, 15].

Here, we show that expression of progerin leads to a rapid loss of RAD51 transcript and protein levels, coinciding with phenotypes of replication fork instability (RFI) and activation of cGAS/STING/IFN cascade. Interestingly, pre-treatment of cells with calcitriol prevents the loss of RAD51, the RFI phenotype, and the activation of the cGAS/STING/IFN pathway upon progerin expression. These results support a key role for the active hormonal form of vitamin D ameliorating the toxic aging effects of progerin.

## Results

### Progerin expression causes replication fork instability that is rescued by calcitriol

In this study, we used a stable cell line of human derived fibroblasts (HDFs) containing a doxycycline-inducible GFP-progerin expression construct to monitor the effects of progerin induction over time [16]. As control, we used HDFs with doxycycline-inducible GFP-lamin A. Doxycycline (1 µg/ml for GFP-progerin and 32 ng/ml for GFP-lamin A) or vehicle were added to HDFs and cells collected every 24 hours to monitor expression of GFP-progerin or GFP-lamin A by immunoblotting (Fig 1A). To test the impact on replication, we performed single-molecule replication analysis (DNA fiber assays). We labeled cells with two thymidine analogs -iododeoxyuridine (IdU) and chlorodeoxyuridine (CldU)- for equal periods of time (20 min), followed by DNA spreading and immunofluorescence to detect newly replicated DNA (Fig 1B). Progressing forks (continuous IdU-CldU label) were scored, the length of red and green tracts measured, and the ratio CldU/IdU calculated. Control cells (not treated with doxycycline) or cells overexpressing GFP-lamin A show similar length of red and green tracts, and an average ratio CldU/IdU of ~1, indicating normal replication fork (RF) progression (Fig 1B). In contrast, expression of GFP-progerin caused shortening of the green tracts and an average ratio CldU/IdU<1, characteristic of replication fork instability (RFI), as early as 24 hours post-induction. This RFI was exacerbated 48 hours after progerin induction. This represent a robust replication stress (RS).

Our previous studies revealed that calcitriol treatment ameliorates many of the aging phenotypes in progerin-expressing cells, including DNA damage and RS [7]. Here, we find that pre-treatment of HDFs with calcitriol for 2 days prior to induction of progerin completely prevents the RFI observed 48 hours after doxycycline treatment (Fig 1C). In particular, DNA fiber assays show that the CldU/IdU ratio is ~1 in progerin-expressing cells treated with calcitriol (Fig 1D). Calcitriol did not have any effect on RF stability in control cells or in cells overexpressing GFP-lamin A (Fig 1E). Our results indicate that calcitriol has the ability to prevent detrimental cellular effects induced by progerin such is the case of replication stress.

### RAD51 downregulation upon progerin expression

To understand the molecular mechanisms underlying RS in progerin-expressing cells, and the mechanisms responsible for the rescue by calcitriol, we monitored the levels of factors with a known role in RF stability and DNA repair. First, we re-analyzed our published RNAseq studies performed in HGPS patient-derived fibroblasts proliferating in culture for three months [7] (accession number: GSE97986) to monitor levels of expression of DNA repair/replication factors. This analysis revealed downregulation of a variety of factors in the BRCA pathway with respect to normal fibroblasts from parents of HGPS patients (Fig 2A). These factors include BRCA1/2, RAD51, and Fanconi Anemia proteins (FANCB/C/D2/E/G/I/M), which play a protective role during RS assisting RF recovery after stalling [17]. RAD51 in particular appeared in our analysis as one of the most downregulated DNA repair factors in HGPS cells, at least at transcripts level. This finding is important because RAD51 plays a key role maintaining the stability of forks during RS, mediating fork

reversal and proper restart of stalled forks. In addition, depletion of RAD51 has been shown to activate cGAS/STING pathway by causing RS and also increasing the amount of ssDNA free in the nucleus and in the cytoplasm [13].

Here, we determined whether RAD51 loss was observed upon induction of progerin expression. As shown in Fig 2B, induction of GFP-progerin results in a marked decrease in RAD51 levels, as early as one day after doxycycline addition, coinciding with RFI (Fig 1B). The downregulation of RAD51 is accompanied by decreased levels of vitamin D receptor (VDR), as previously reported in progerin-expressing cells [6], and followed by increased levels of phosphorylated RPA on residue Ser33 (P-RPA<sup>S33</sup>), a marker of RS. Furthermore, we find that expression of progerin does lead to increased levels of cGAS, STING, and ISG15, as previously reported [7]. The decrease in RAD51 and the increase in P-RPA<sup>S33</sup> were recapitulated by immunofluorescence performed 4 days after progerin induction (Fig 2C). To determine if the downregulation of RAD51 was at the level of transcription, we performed qRT-PCR during the progerin-induction protocol. As shown in Fig 2D, RAD51 transcripts levels exhibit a gradual decrease during the induction of progerin expression.

Altogether, these data demonstrate a marked downregulation of RAD51 at transcript and protein levels in progerin-expressing cells, concomitant with an increase in P-RPA<sup>S33</sup>, a marker of RS. This suggests a potential deficiency in the switch between P-RPA and RAD51 during RS in progerin-expressing cells, which could hinder RF protection from nucleases, as well as RF reversal and restart, all key functions of RAD51.

Next, we monitored the levels and localization of 53BP1, a key factor in DNA repair by non-homologous end-joining, previously shown to be degraded during extended proliferation of HGPS cells in culture [6]. We did not find alterations in the levels of 53BP1 (Fig 3A) or its ability to form foci at sites of DNA damage induced by progerin (Fig 3B) in this inducible cellular system. Moreover, we tested whether oxidative stress, known to be increased in progeria cells, could be contributing to RAD51 loss. Our previous studies in primary fibroblasts subjected to a long protocol of H<sub>2</sub>O<sub>2</sub> treatment that causes oxidative stress-induced senescence revealed a marked downregulation of RAD51 [18]. However, acute treatment with H<sub>2</sub>O<sub>2</sub> at a concentration that causes oxidative stress and DNA damage but not cell senescence or death [19] results in no changes in RAD51 levels in either control or progerin-expressing cells (Fig 3C). This treatment with H<sub>2</sub>O<sub>2</sub> did increase the levels of 53BP1 nuclear foci, consistent with accumulation of DNA damage (Fig 3D). Thus, we conclude that low levels of oxidative stress do not reduce RAD51 expression, but the high levels that induce senescence are associated with RAD51 loss. Additional studies will be required to determine if RAD51 reduction during oxidative stress-induced senescence is due to oxidative stress or the inhibition of replication/proliferation.

### **Calcitriol increases RAD51 expression and prevents cGAS/STING/IFN activation in progerin-expressing cells**

We previously showed that calcitriol represses the STAT1-mediated IFN-like response in HGPS patient derived fibroblasts [7]. Specifically, the expression of about 50 genes in the IFN/antiviral/innate immunity category upregulated in HGPS fibroblasts, was normalized by calcitriol (accession number: GSE97986). In addition, calcitriol treatment rescues RFI in



The mechanism behind the repression of RAD51 expression by progerin and the rescue by calcitriol is not known. In lamin A/C-depleted cells, we reported that reduced expression of RAD51 is mediated by a repressor complex consisting of the Retinoblastoma (Rb) family member p130 and the transcription factor E2F4 [24]. Whether or not this is the mechanism in progerin-expressing cells remains to be determined. A recurrent observation in our studies is that the levels of expression of RAD51 are tightly linked to the levels of VDR in a variety of contexts. Depletion of VDR in normal human fibroblasts results in downregulation of RAD51 and a rapid growth arrest with characteristics of senescence [18]. During oncogenic Ras-induced senescence, we find a marked repression of RAD51, concomitant with VDR downregulation, and calcitriol treatment upregulates VDR and increases RAD51 levels [6]. Thus, it is tempting to speculate that VDR is regulating RAD51 transcription either directly or indirectly.

Moreover, direct links have been established between the levels of expression of RAD51 and the status of the cGAS-STING-IFN pathway [13]. In particular, RAD51 and RPA ssDNA-binding proteins have been proposed to act as nuclear retainers of nucleic acid byproducts of DNA damage generated during replication stress. Under conditions of limited genomic instability, RAD51 and RPA are sufficient to sequester the ssDNA fragments generated in the nucleus, preventing its leakage into the cytoplasm. However, if genomic instability is severe or persistent, the saturation of RAD51 and RPA leads to accumulation of cytoplasmic ssDNA, which in turn triggers cGAS-dependent IFN activation [13]. Thus, in the case of progerin-expressing cells, it is possible that the loss of RAD51 contributes to the accumulation of ssDNA in the cytoplasm, which together with increased nuclear fragility and DNA damage might drive the robust activation of cGAS-STING-IFN response.

Importantly, this study demonstrates a robust effect of calcitriol, hormonal active form of vitamin D, repressing the cGAS-STING-IFN response. Although our previous studies showed this effect in HGPS fibroblasts cultured in the presence of calcitriol for a long period of time (~90 days) when compared to normal fibroblasts [2, 4, 6], now we are able to monitor the activation/repression of these pathways over time. In fact, we find that pre-treatment of cells with calcitriol prevents RAD51 loss, replication stress, and activation of cGAS-STING-IFN pathway upon progerin expression. These findings are relevant, as they add to the numerous beneficial effects observed by calcitriol treatment in progeria cells, which include normalization of nuclear morphology and size, reduced DNA damage accumulation, improved proliferation, and delayed senescence [6]. However, many questions remain to be addressed with respect to mechanisms underlying calcitriol benefits. For instance, it is possible that by reducing DNA damage/replication stress, calcitriol reduces leakage of DNA into the cytoplasm and activation of cGAS-STING and the downstream STAT1-IFN response. Alternatively, it is possible that calcitriol, via VDR, represses the expression of genes in the STAT1-IFN cascade, independent of genomic instability. In fact, some studies found that STAT1 and STAT3 are constitutively active and hyperphosphorylated in some leukemias and that VDR pathway activation deactivates STAT proteins and inflammatory cytokine production [25]. Thus, the active form of vitamin D -calcitriol- and its analogs have gained much recognition as immune regulators, although much of the data relates to T cells. Further studies are needed to define in detail the mechanisms underlying the robust effect of calcitriol reducing RFI and repressing the cGAS-STING-IFN response in HGPS and other

progerin-expressing cells. Also, preclinical studies with mouse models of progeria are necessary to determine if the aging phenotype of these mice is delayed or ameliorated by calcitriol.

## Materials and Methods

### Cell Culture

Human derived fibroblasts (HDFs) containing doxycycline-inducible GFP-progerin or GFP-lamin A constructs were maintained in culture as described [26], and treated with doxycycline (1  $\mu\text{g}/\text{ml}$  for GFP-progerin and 32  $\text{ng}/\text{ml}$  for GFP-lamin A) or vehicle as control for the indicated times (1–4 days). Calcitriol (1 $\alpha$ ,25-dihydroxyvitamin D<sub>3</sub>), the hormonal active form of vitamin D, was added to cells either 2 days prior or together with doxycycline at a concentration of  $10^{-7}$  M. To induce oxidative stress, HDFs that had been growing in media containing doxycycline or vehicle for 2 days were exposed to 100  $\mu\text{M}$  H<sub>2</sub>O<sub>2</sub> for 2 hours. This treatment has been shown to induce oxidative stress [19].

### Immunoblotting and Immunofluorescence

**Immunoblotting**—Cells were lysed in UREA buffer (8 M Urea, 40 mM Tris pH7.5, 1% NP40) for 20 min on ice, and 60–120  $\mu\text{g}$  of total protein was loaded on 4–15% Criterion-TGX-Gel (Bio-Rad).

**Immunofluorescence**— $3 \times 10^5$  cells were fixed in 3.7% formaldehyde+0.2% Triton-X100 in PBS for 10 minutes, washed 3X in PBS, and blocked 1 hour at 37°C in 10% BSA/PBS. Incubations with antibodies were performed for 1 hour at 37°C, in a humid chamber. After washes in PBS, cells were counterstained with DAPI in Vectashield. Microscopy and photo capture were performed on a Leica DM5000 B microscope using 40x or 63x oil objective lenses with a Leica DFC350FX digital camera and the Leica Application Suite.

### Quantitative Reverse-Transcription PCR

cDNA was generated by reverse transcription of 1  $\mu\text{g}$  total RNA using GeneAmp® RNA PCR kit. qRT-PCR was performed using the 7500HT Fast Real-Time PCR system with the Taqman® Universal PCR Master Mix or Universal SYBR Green Supermix. Reactions were carried out in triplicate and target gene and endogenous controls amplified in the same plate. Relative quantitative measurements of target genes were determined by comparing cycle thresholds.

### DNA Fiber Assays

Fiber assays were performed on normal human derived fibroblasts (HFDs) and HDFs induced to express GFP-progerin or GFP-lamin A via addition of doxycycline. Asynchronous cells were labeled for 20 min each with two thymidine analogs: 20  $\mu\text{M}$  iododeoxyuridine (IdU) followed by 200  $\mu\text{M}$  chlorodeoxyuridine (CldU). Cells were collected by trypsinization, washed and resuspended in 100  $\mu\text{l}$  of PBS. Then, 2  $\mu\text{l}$  cell suspension was dropped on a polarized slide (Denville Ultraclear) and cell lysis was performed in situ by adding 8  $\mu\text{l}$  of lysis buffer (200 mM Tris-HCl pH7.5; 50 mM EDTA; 0.5% SDS). Stretching of high-molecular weight DNA was achieved by tilting the slides at

15–45°. The resulting DNA spreads were air dried and fixed for 5 min in 3:1 Methanol:Acetic acid and refrigerated overnight. For immunostaining, stretched DNA fibers were denatured with 2.5 N HCl for 60 min, washed 3X in PBS, then blocked with 5% BSA in PBS for 30 min at 37°C. Rat anti-CldU/BrdU (Abcam, ab6326) (1:100), chicken anti-rat Alexa 488 (Invitrogen, A21470) (1:100), mouse anti-IdU/BrdU (BD Biosciences, 347580) (1:20) and goat anti-mouse IgG1 Alexa 547 (Invitrogen, A21123) (1:100) antibodies were used to reveal CldU- and IdU-labeled tracts, respectively. A Leica SP5X confocal microscope was used to visualize the labeled tracts, and tract lengths were measured using ImageJ (<http://rsbweb.nih.gov/beckersproxy.wustl.edu/ij/>). Statistical analysis of the tract length was performed using GraphPad Prism (<http://www.graphpad.com/scientific-software/prism/>).

## RNAseq

The detailed RNAseq procedure is described in [7]. In this study, we compared the levels of DNA repair factors between three lines of normal fibroblasts (from parents of patients with HGPS) and three different lines of HGPS fibroblasts that had been growing in culture for 90 days in complete normal media.

## Statistical Analysis

For all qRT-PCR experiments, a standard “two-tailed” student’s t-test was used to calculate statistical significance of the observed differences. For DNA fiber experiments, unpaired two-tailed t-test with Welch-correction for unequal distribution was performed. We utilized GraphPad Prism software for all statistical analyses. In all cases, differences were considered statistically significant when  $p < 0.05$  (\* $p < 0.05$ , \*\* $p < 0.01$ , \*\*\* $p < 0.001$ , \*\*\*\* $p < 0.0001$ ).

Antibodies used for immunoblotting	Antibody (Dilution)
Lamin A	ab26300, Abcam (1:1000)
Progerin	SAB4200272, Sigma-Aldrich (1:1000)
Lamin A/C	sc-20681, SCBT (1:2000)
VDR	sc-13133, SCBT (1:200)
$\beta$ -Tubulin	T8238, Sigma Aldrich (1:2000)
STAT1	#9172, Cell Signaling (1:1000)
P-STAT1 (Y701)	#7649, Cell Signaling (1:1000)
P-STAT1 (S727)	#9177, Cell Signaling (1:1000)
P-RPA	A300–245A, Bethyl Laboratories (1:1000)
ISG15	sc-166755, SCBT (1:1000)
cGAS	#D1D3G, Cell Signaling (1:300)
STING	#D2P2F, Cell Signaling (1:1000)
RAD51	#PC130, Calbiochem (1:1000)
53BP1	#22760, SCBT (1:1000)
Antibodies used for immunofluorescence	Antibody



P-RPA	A300–245A, Bethyl Laboratories (1:1000)
RAD51	#PC130, Calbiochem (1:1000)
53BP1	#22760, SCBT (1:400)

## Acknowledgments

We are in debt with Nard Kubben and Tom Misteli (NIH) for sharing the cell lines. Research in the laboratory of S.G. was supported by NIA Grant RO1 AG058714.

## Abbreviations

<b>HGPS</b>	Hutchinson Gilford Progeria Syndrome
<b>LMNA</b>	lamin A gene
<b>RS</b>	replication stress
<b>RF</b>	replication fork
<b>IFN</b>	interferon
<b>STAT</b>	signal transducer and activator of transcription
<b>VDR</b>	vitamin D receptor
<b>cGAS</b>	cyclic GAMP synthase
<b>STING</b>	stimulator of interferon genes

## References

- [1]. Gonzalo S, Kreienkamp R, Askjaer P, Ageing Res Rev 2017, 33, 18 [PubMed: 27374873] Lattanzi G, Maggi L, Araujo-Vilar D, Nucleus 2018, 9, 543 [PubMed: 30719953] Brull A, Morales Rodriguez B, Bonne G, Muchir A, Bertrand AT, Front Physiol 2018, 9, 1533. [PubMed: 30425656]
- [2]. Kreienkamp R, Gonzalo S, Subcell Biochem 2019, 91, 435. [PubMed: 30888661]
- [3]. Wu Z, Wu L, Weng D, Xu D, Geng J, Zhao F, J Exp Clin Cancer Res 2009, 28, 8 [PubMed: 19144202] Belt EJ, Fijneman RJ, van den Berg EG, Brill H, Delis-van Diemen PM, Tijssen M, van Essen HF, de Lange-de Klerk ES, Belien JA, Stockmann HB, Meijer S, Meijer GA, Eur J Cancer 2011, 47, 1837 [PubMed: 21621406] Wang Y, Jiang J, He L, Gong G, Wu X, Gynecol Oncol 2019, 152, 166 [PubMed: 30384980] Agrelo R, Setien F, Espada J, Artiga MJ, Rodriguez M, Perez-Rosado A, Sanchez-Aguilera A, Fraga MF, Piris MA, Esteller M, J Clin Oncol 2005, 23, 3940 [PubMed: 15867203] Kaspi E, Frankel D, Guinde J, Perrin S, Laroumagne S, Robaglia-Schlupp A, Ostacolo K, Harhour K, Tazi-Mezalek R, Micallef J, Dutau H, Tomasini P, De Sandre-Giovannoli A, Levy N, Cau P, Astoul P, Roll P, PLoS One 2017, 12, e0183136 [PubMed: 28806747] Alhudiri IM, Nolan CC, Ellis IO, Elzagheid A, Rakha EA, Green AR, Chapman CJ, Breast Cancer Res Treat 2019.
- [4]. Graziano S, Kreienkamp R, Coll-Bonfill N, Gonzalo S, Nucleus 2018, 9, 258. [PubMed: 29637811]
- [5]. Dobrzynska A, Gonzalo S, Shanahan C, Askjaer P, Nucleus 2016, 0; S. Gonzalo, R. Kreienkamp, Curr Opin Cell Biol 2015, 34, 75Gonzalo S, Adv Exp Med Biol 2014, 773, 377. [PubMed: 24563357]

- [6]. Kreienkamp R, Croke M, Neumann MA, Bedia-Diaz G, Graziano S, Dusso A, Dorsett D, Carlberg C, Gonzalo S, Oncotarget 2016.
- [7]. Kreienkamp R, Graziano S, Coll-Bonfill N, Bedia-Diaz G, Cybulla E, Vindigni A, Dorsett D, Kubben N, Batista LFZ, Gonzalo S, Cell Rep 2018, 22, 2006. [PubMed: 29466729]
- [8]. Hilton BA, Liu J, Cartwright BM, Liu Y, Breitman M, Wang Y, Jones R, Tang H, Rusinol A, Musich PR, Zou Y, FASEB J 2017, 31, 3882Wheaton K, Campuzano D, Ma W, Sheinis M, Ho B, Brown GW, Benchimol S, Mol Cell Biol 2017, 37.
- [9]. Tang H, Hilton B, Musich PR, Fang DZ, Zou Y, Aging Cell 2012, 11, 363. [PubMed: 22168243]
- [10]. Ng KW, Marshall EA, Bell JC, Lam WL, Trends Immunol 2018, 39, 44Bakhoum SF, Ngo B, Laughney AM, Cavallo JA, Murphy CJ, Ly P, Shah P, Sriram RK, Watkins TBK, Taunk NK, Duran M, Pauli C, Shaw C, Chadalavada K, Rajasekhar VK, Genovese G, Venkatesan S, Birkbak NJ, McGranahan N, Lundquist M, LaPlant Q, Healey JH, Elemento O, Chung CH, Lee NY, Imielski M, Nanjangud G, Pe'er D, Cleveland DW, Powell SN, Lammerding J, Swanton C, Cantley LC, Nature 2018, 553, 467 [PubMed: 29342134] Wang H, Hu S, Chen X, Shi H, Chen C, Sun L, Chen ZJ, Proc Natl Acad Sci U S A 2017, 114, 1637; Ablasser A, Chen ZJ, Science 2019, 363. [PubMed: 28137885]
- [11]. Li T, Chen ZJ, J Exp Med 2018, 215, 1287. [PubMed: 29622565]
- [12]. Ahn J, Xia T, Konno H, Konno K, Ruiz P, Barber GN, Nat Commun 2014, 5, 5166 [PubMed: 25300616] Bhattacharya S, Srinivasan K, Abdisalaam S, Su F, Raj P, Dozmorov I, Mishra R, Wakeland EK, Ghose S, Mukherjee S, Asaithamby A, Nucleic Acids Res 2017, 45, 4590 [PubMed: 28334891] Harding SM, Benci JL, Irianto J, Discher DE, Minn AJ, Greenberg RA, Nature 2017, 548, 466. [PubMed: 28759889]
- [13]. Wolf C, Rapp A, Berndt N, Staroske W, Schuster M, Dobrick-Mattheuer M, Kretschmer S, Konig N, Kurth T, Wieczorek D, Kast K, Cardoso MC, Gunther C, Lee-Kirsch MA, Nat Commun 2016, 7, 11752. [PubMed: 27230542]
- [14]. Dou Z, Ghosh K, Vizioli MG, Zhu J, Sen P, Wangenstein KJ, Simithy J, Lan Y, Lin Y, Zhou Z, Capell BC, Xu C, Xu M, Kieckhaefer JE, Jiang T, Shoshkes-Carmel M, Tanim K, Barber GN, Seykora JT, Millar SE, Kaestner KH, Garcia BA, Adams PD, Berger SL, Nature 2017, 550, 402 [PubMed: 28976970] Chen Q, Sun L, Chen ZJ, Nat Immunol 2016, 17, 1142 [PubMed: 27648547] Sun L, Wu J, Du F, Chen X, Chen ZJ, Science 2013, 339, 786. [PubMed: 23258413]
- [15]. Lee S, Schmitt CA, Nat Cell Biol 2019, 21, 94. [PubMed: 30602768]
- [16]. Kubben N, Brimacombe KR, Donegan M, Li Z, Misteli T, Methods 2016, 96, 46. [PubMed: 26341717]
- [17]. Palovcak A, Liu W, Yuan F, Zhang Y, Cell Biosci 2017, 7, 8. [PubMed: 28239445]
- [18]. Graziano S, Johnston R, Deng O, Zhang J, Gonzalo S, Oncogene 2016.
- [19]. Bhatia V, Valdes-Sanchez L, Rodriguez-Martinez D, Bhattacharya SS, F1000Res 2018, 7, 1233. [PubMed: 30345028]
- [20]. Scully R, Chen J, Plug A, Xiao Y, Weaver D, Feunteun J, Ashley T, Livingston DM, Cell 1997, 88, 265 [PubMed: 9008167] Zhang H, Tomblin G, Weber BL, Cell 1998, 92, 433. [PubMed: 9491884]
- [21]. Kowalczykowski SC, Cold Spring Harb Perspect Biol 2015, 7.
- [22]. Hashimoto Y, Ray Chaudhuri A, Lopes M, Costanzo V, Nat Struct Mol Biol 2010, 17, 1305. [PubMed: 20935632]
- [23]. Zellweger R, Dalcher D, Mutreja K, Berti M, Schmid JA, Herrador R, Vindigni A, Lopes M, J Cell Biol 2015, 208, 563. [PubMed: 25733714]
- [24]. Redwood AB, Perkins SM, Vanderwaal RP, Feng Z, Biehl KJ, Gonzalez-Suarez I, Morgado-Palacin L, Shi W, Sage J, Roti-Roti JL, Stewart CL, Zhang J, Gonzalo S, Cell Cycle 2011, 10, 2549. [PubMed: 21701264]
- [25]. Olson KC, Kulling Larkin PM, Signorelli R, Hamele CE, Olson TL, Conaway MR, Feith DJ, Loughran TP Jr., Cytokine 2018, 111, 551. [PubMed: 30455079]
- [26]. Kubben N, Zhang W, Wang L, Voss TC, Yang J, Qu J, Liu GH, Misteli T, Cell 2016, 165, 1361. [PubMed: 27259148]

### Statement of significance

In this study, we use an inducible system of expression of progerin in human fibroblasts to dig into molecular mechanisms underlying its well-known cellular toxicity. We find that only one to two days after progerin induction, cells recapitulate phenotypes previously identified in HGPS patients derived fibroblasts, namely replication stress and activation of cGAS/STING pathway and STAT1/IFN-like response. The fast effect of progerin triggering these responses suggests that they might be at the root of cellular decline and serve as potential targets to mitigate downstream detrimental effects. Moreover, we show for the first time that progerin elicits a marked downregulation of RAD51, a crucial factor in DNA repair and replication fork stability. Interestingly, calcitriol upregulates RAD51, rescues progerin-induced replication stress and represses the cGAS/STING/STAT1/IFN cascade, suggesting a functional relationship among these progerin-induced alterations and a strategy to reduce progerin toxicity in cells.

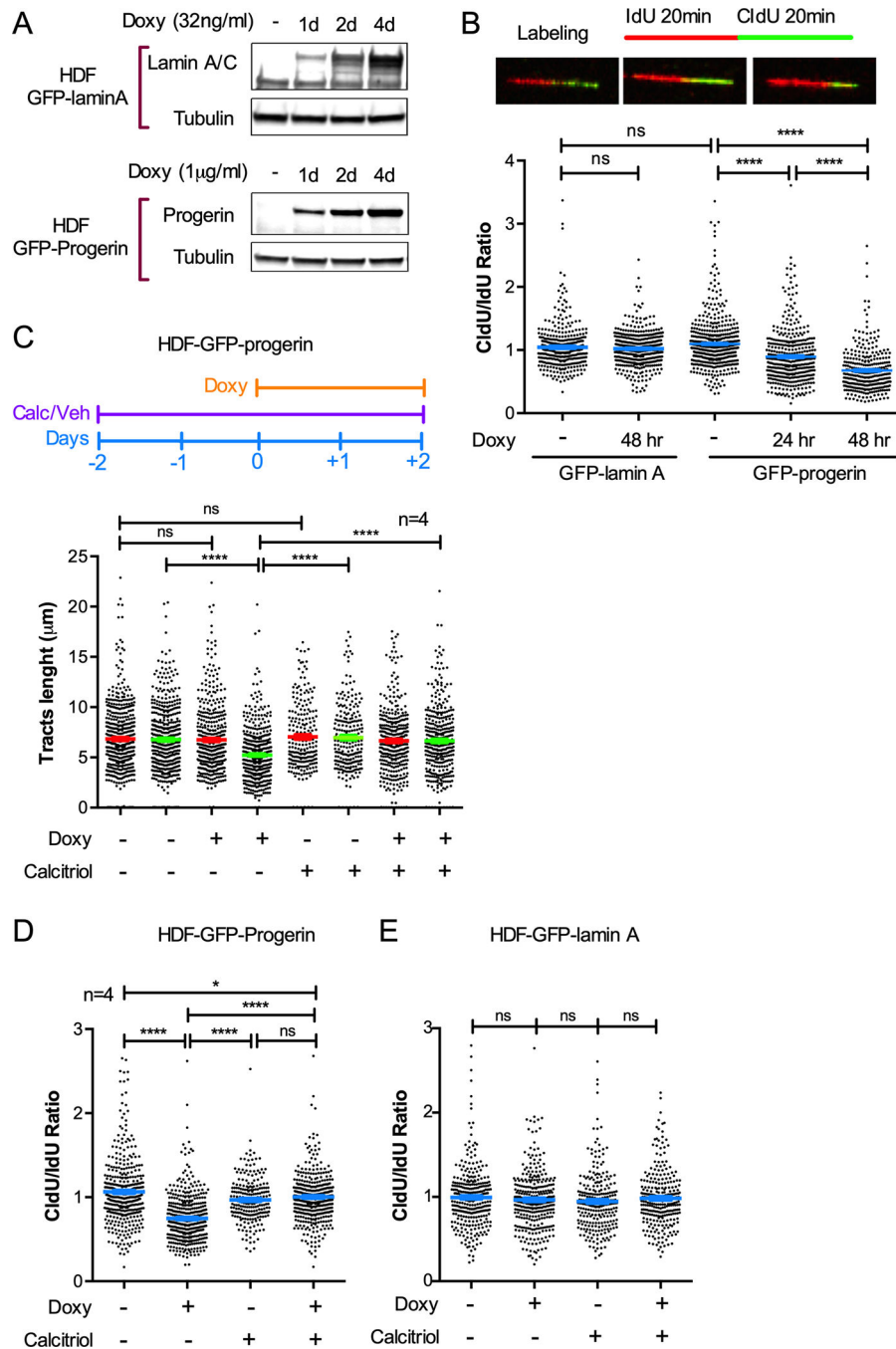


**Figure 1. Expression of progerin causes replication fork instability that is rescued by calcitriol.** (A) Immunoblots showing induction of expression of GFP-lamin A or GFP-progerin in human derived fibroblasts (HDF) via treatment with doxycycline (Doxy) for increasing number of days. Lamin A/C antibody shows increasing levels of GFP-lamin A, while endogenous lamin A levels remain constant.  $\beta$ -tubulin is the loading control. (B) Single-molecule replication analysis performed in HDF described in (A). Images show DNA fibers in GFP-progerin cells labeled with IdU 20 min + CldU 20 min as detected by fluorescence confocal microscopy. Left: no Doxy; Central: Doxy 24 hr.; Right: Doxy 48 hr. Tract lengths

are measured using ImageJ. Graph shows the tract length ratio CldU/IdU in untreated HDF and Doxy-treated cells for 24 and 48 hr. Note how the ratio CldU/IdU is  $<1$  in GFP-progerin but not in GFP-lamin A cells. Graph shows average  $\pm$  s.e.m. of 3 biological repeats (3 independent treatments). (C) HDF-GFP-progerin cells were treated with calcitriol (100 nM  $1\alpha,25$ -dihydroxy-vitamin  $D_3$ ) for 2 days prior to induction of GFP-progerin by Doxy. The lengths of red and green tracts under the different conditions are shown. Graph shows average  $\pm$  s.e.m. of 4 biological repeats (4 independent treatments). Note how green tract shortening in GFP-progerin-expressing cells is rescued by calcitriol. (D) Tract length ratio CldU/IdU in HDF-GFP-progerin cells. (E) CldU/IdU ratio in HDF-GFP-lamin A cells. ~100 fibers measured in each experiment. All DNA fiber assays were performed with the same labeling scheme as in (A), and statistical differences were considered significant if  $p < 0.05$ .

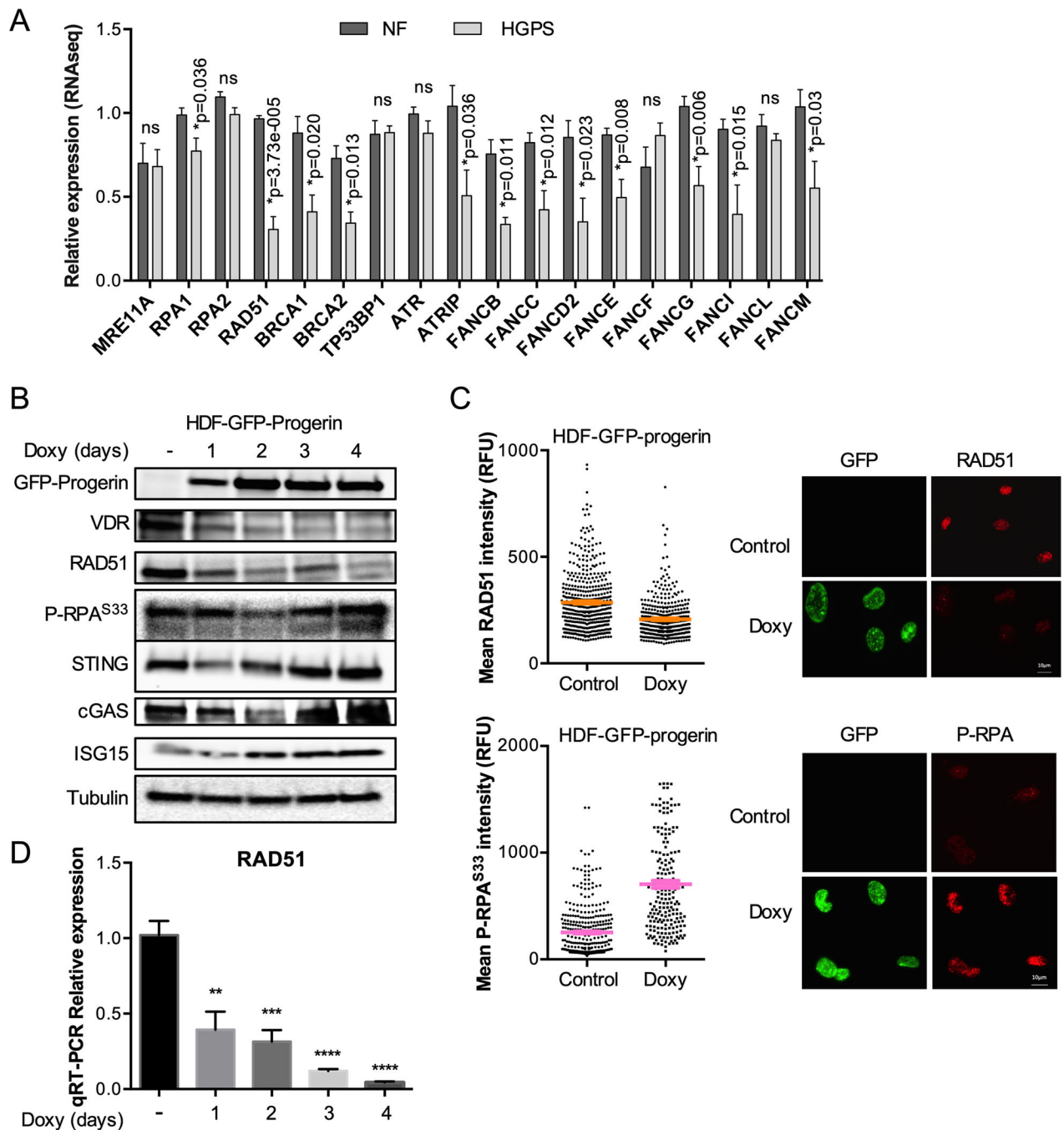


**Figure 2. Progerin causes downregulation of RAD51.**

(A) Re-analysis of published RNAseq data performed in 5 lines of normal fibroblasts (NF) and 3 lines of HGPS patients-derived fibroblasts growing in culture for 90 days [7] (accession # GSE97986). Expression of DNA repair genes shows a decrease in the BRCA pathway. \*p represents p-value of statistical significance and ns=no significant ( $p>0.05$ ). (B) HDF-GFP-Progerin cells were treated with Doxy for increasing days and the levels of RAD51, P-RPA<sup>S33</sup>, VDR, and proteins in the cGAS/STING/IFN pathway monitored by immunoblotting.  $\beta$ -tubulin is the loading control. (C) Immunofluorescence in HDF-GFP-

progerin cells treated with Doxy for 4 days. Graphs show quantitation of RAD51 (top) and P-RPA<sup>S33</sup> (bottom) labeling intensity (relative fluorescence units). GFP staining was used to demarcate nuclei and intensity of RAD51 and P-RPA<sup>S33</sup> labeling measured using ImageJ program. Results are the average  $\pm$  s.e.m. of 3 independent experiments. **(D)** Relative expression of RAD51 transcripts by qRT-PCR in HDF-GFP-Progerin cells treated with Doxy for increasing days. Results are average  $\pm$  s.e.m. of 2 biological repeats, each performed in triplicate.

Author Manuscript

Author Manuscript

Author Manuscript

Author Manuscript

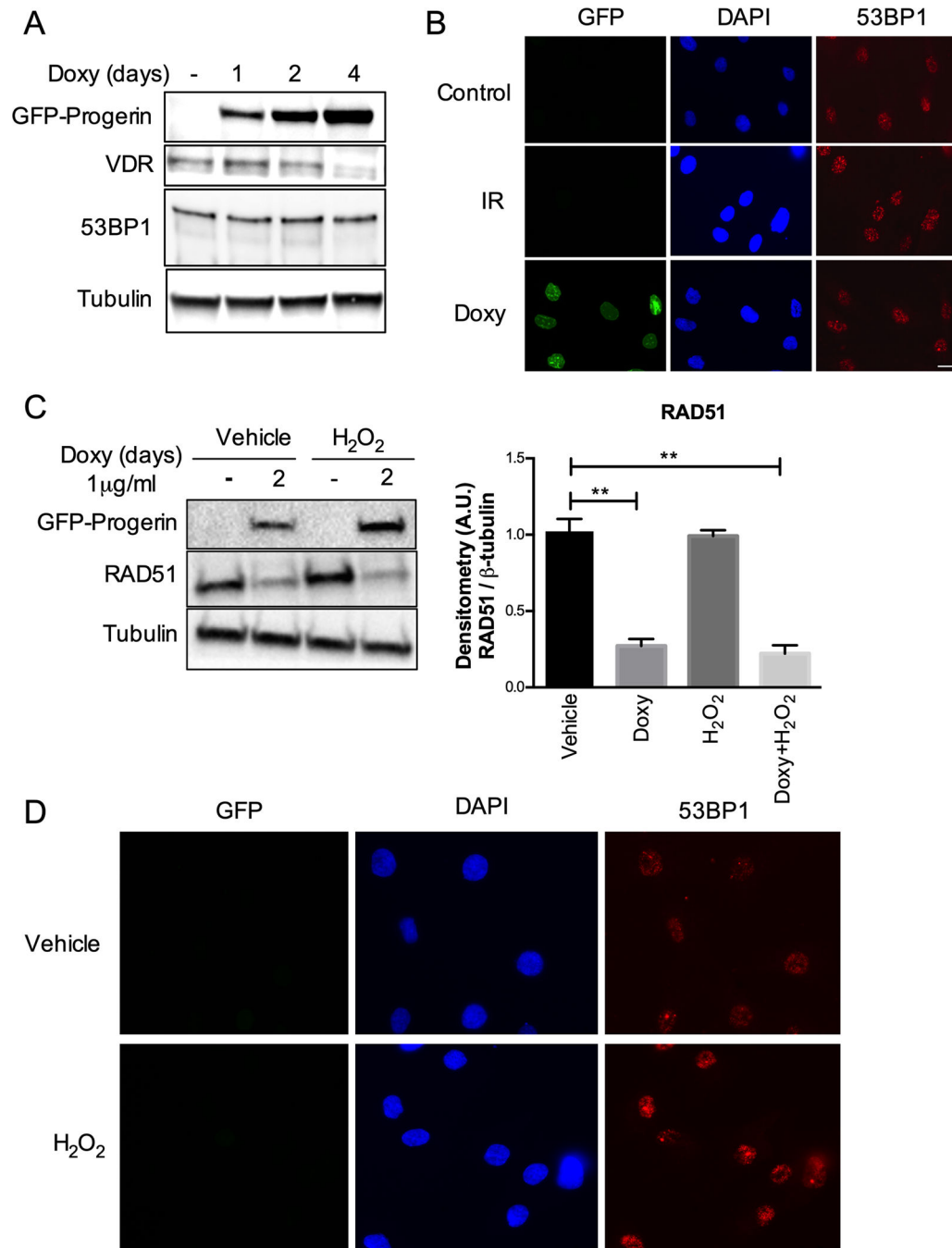


**Figure 3. Effects of progerin on 53BP1 and of oxidative stress on RAD51.**

(A) HDF-GFP-progerin cells induced to express progerin with Doxy for 1–4 days. The levels of VDR and 53BP1 are shown, with  $\beta$ -tubulin as loading control. Note the constant levels of 53BP1 upon progerin expression. (B) Immunofluorescence to monitor behavior of 53BP1. Control cells (not irradiated) show normal levels of 53BP1, which accumulate at foci of DNA damage upon ionizing radiation (IR). In progerin-expressing cells (Doxy), 53BP1 forms foci representing most likely recruitment of the protein to sites of DNA damage. (C) HDF-GFP-progerin cells treated with H<sub>2</sub>O<sub>2</sub> and levels of RAD51 protein monitored by



immunoblotting. Graph shows quantitation of densitometry of three biological repeats (average  $\pm$  s.e.m.). Note the marked downregulation of RAD51 by doxycycline treatment (progerin expression) but not by H<sub>2</sub>O<sub>2</sub> exposure. **(D)** Immunofluorescence in HDFs not expressing progerin but treated with H<sub>2</sub>O<sub>2</sub> shows increased 53BP1 foci, consistent with oxidative stress causing DNA damage.

Author Manuscript

Author Manuscript

Author Manuscript

Author Manuscript

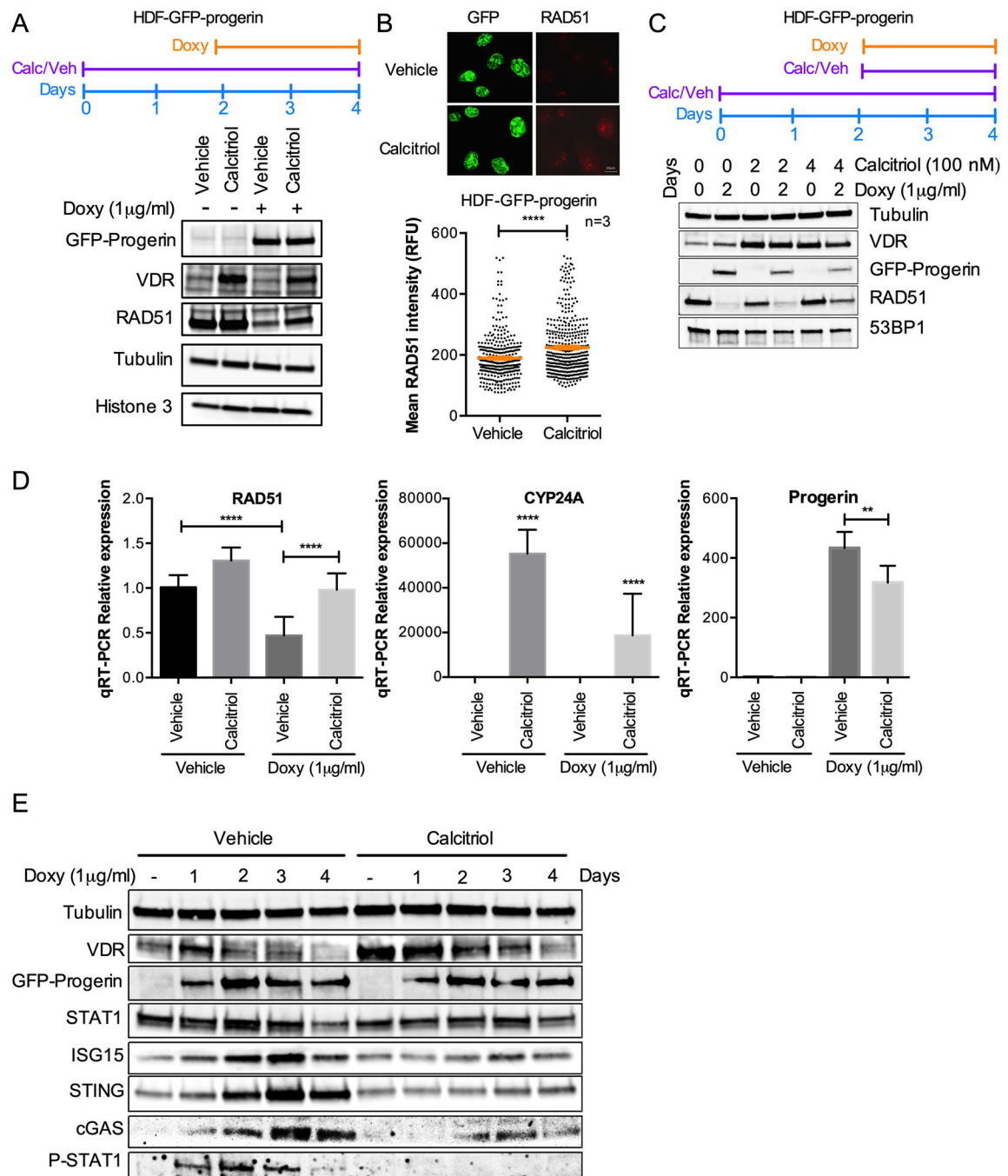


**Figure 4. Calcitriol prevents RAD51 loss and cGAS/STING/IFN activation caused by progerin.** (A) HDF-GFP-progerin cells were treated with calcitriol (100nM 1 $\alpha$ ,25-dihydroxy-vitamin D<sub>3</sub>) for 2 days prior to induction of GFP-progerin by Doxy. The levels of VDR and RAD51 under the different conditions are shown. Note how the decrease in RAD51 upon progerin expression is partly rescued by calcitriol.  $\beta$ -tubulin and histone H3 used as loading control. (B) Immunofluorescence in HDF-GFP-progerin cells treated with calcitriol or vehicle 2 days prior to Doxy induction of GFP-progerin for 4 days. Graph shows quantitation of RAD51 labeling intensity (relative fluorescence units), as measured by ImageJ program. GFP

staining was used to demarcate nuclei. Results are the average  $\pm$  s.e.m. of 3 independent experiments. (C) HDF-GFP-progerin cells were pre-treated with calcitriol (100 nM) for 2 days prior to induction of GFP-progerin by Doxy or treated with both calcitriol and Doxy at the same time. The levels of VDR and RAD51 under the different conditions are shown. Note how the pre-treatment with calcitriol is necessary to partially prevent RAD51 loss upon progerin expression.  $\beta$ -tubulin used as loading control. 53BP1 levels are also constant in the different conditions. (D) Relative expression of RAD51, CYP24A, and progerin-specific transcripts by qRT-PCR in HDF-GFP-Progerin cells pretreated with calcitriol or vehicle for 2 days followed by Doxy or vehicle for 4 days. Results are average  $\pm$  s.e.m. of 2 biological repeats, each performed in triplicate. (E) HDF-GFP-Progerin cells were pretreated with calcitriol or vehicle for 2 days, followed by Doxy for increasing days. Activation of cGAS/STING/IFN pathway monitored by immunoblotting.  $\beta$ -tubulin is the loading control. VDR shows the effect of calcitriol. Note the robust effect of calcitriol preventing the upregulation of cGAS, STING, STAT1, P-STAT1 and ISG15.